Bioinspired Hydroxyapatite/Poly(methyl methacrylate) Composite with a Nacre-Mimetic Architecture by a Bidirectional Freezing Method

Hao Bai, Flynn Walsh, Bernd Gludovatz, Benjamin Delattre, Caili Huang, Yuan Chen, Antoni P. Tomsia, and Robert O. Ritchie**

Lightweight structural materials that are strong and tough are required for many strategic applications in the energy, transportation, construction, and biomedical industries.[1–7] To this end, ceramics are attractive candidate materials due to their high specific strength and temperature resistance, although their application as structural materials has been largely limited by their brittleness and flaw sensitivity.[8] Many biological composites with high ceramic content, however, such as bone and nacre, provide possible design solutions to this problem.[6,9] These materials are primarily composed of brittle minerals (ceramics), such as hydroxyapatite in bone or aragonite in nacre, glued together with a small amount of biopolymer; despite such seemingly meager constituents, these natural low density composites can display unprecedented strength and toughness properties. This can be attributed to their complex, hierarchical architectures assembled from atomistic to near macroscopic scales. Mimicking the structural features of these natural composites has proven to be a promising route to developing potentially new structural materials with superior mechanical performance.

In particular, during the past decade, various methods have been utilized to create nacre-mimetic composites with hierarchical "brick-and-mortar" architectures.[7,10–15] Although much progress has been achieved in this field, it still remains a challenge to precisely control the architectural features over multiple length-scales in materials with high ceramic content, especially when scaled-up for practical applications. For example, slip/tape casting and hot pressing,[16] or recently developed spraying methods,[17] generally lack structural manipulation at the nano- to microscales. Other methods, such as layer-by-layer assembly and vacuum-assisted filtration are usually limited to thin films or micro-sized samples.[2,11,16] On the other hand, freeze casting[4] (also known as ice-templating) has proven to be a powerful technique to produce bulk composites with nacre-mimetic structures that can possess excellent mechanical properties.[5,18,19] By infiltrating freeze-cast alumina scaffolds with poly(methyl methacrylate) (PMMA) as a compliant layer, bending strengths of ≈210 MPa with remarkable fracture toughnesses have been achieved that exceed a stress intensity of 30 MPa $m^{1/2}$ (≈8000 J m^{-2} in energy terms).[5] A similar processing strategy has been applied to other material systems, such as silicon carbide/PMMA composites for high toughness lamellar structures,[19] and an alumina/glass combination for higher temperature (600 °C) applications.[18]

Controlling the precise microstructures, however, in particular the lamellar orientation over larger than centimeter dimensions, has proven to be difficult with conventional freeze casting. Under the single, perpendicular temperature gradient of the cold finger, a consistent orientation of the lamellar structure has only been achieved over multiple submillimeter domains when observed in the cross section perpendicular to the freezing direction.[20] This limitation has long hindered larger-scale fabrication of freeze-cast structures. Although freezing with a patterned cold finger[20] or "freeze under flow" methods[21] have been used to further control the ice crystal nucleation and growth during freezing, they are still limited by sample size and slurry particle shape.

Recently, we have developed a bidirectional freezing technique capable of assembling small building blocks (ceramic particles, platelets, and/or polymer) into large-sized (centimeter-scale), single domain, porous lamellar structures comparable with natural nacre, specifically by introducing a polydimethylsiloxane (PDMS) wedge between the cold finger and the slurry.[22] In the present work, we show as a proof of concept that a hydroxyapatite (HA) scaffold with long-range aligned lamellar structure prepared by bidirectional freezing can be further densified and infiltrated with a compliant layer (PMMA) to generate a nacre-mimetic composite as large as 4 × 8 × 25 mm (currently limited by the size of the mold, although theoretically scalable). This composite can reach ceramic contents as high as 75–85 vol% which was controlled by pressing the scaffold to different thicknesses; in comparison to its constituent materials, it displays an excellent combination of mechanical properties of an elastic modulus on the order of 20 GPa, a bending strength of ≈100 MPa, with a work of fracture as high as 2075 J m^{-2} (some 100 times higher than monolithic HA).[23] Hydroxyapatite is not

Prof. H. Bai,[+] F. Walsh, Dr. B. Gludovatz, B. Delattre, Dr. C. Huang, Dr. Y. Chen, Dr. A. P. Tomsia, Prof. R. O. Ritchie
Materials Sciences Division
Lawrence Berkeley National Laboratory
Berkeley, CA 94720, USA
E-mail: hbai@zju.edu.cn; roritchie@lbl.gov
B. Delattre
Laboratoire de Physique des Surfaces et Interfaces
Université de Mons
Mons 7000, Belgium
Prof. R. O. Ritchie
Department of Materials Science and Engineering
University of California
Berkeley, CA 94720, USA
[+]Present address: State Key Laboratory of Chemical Engineering, College of Chemical and Biological Engineering, Zhejiang University, Hangzhou 310027, China

DOI: 10.1002/adma.201504313

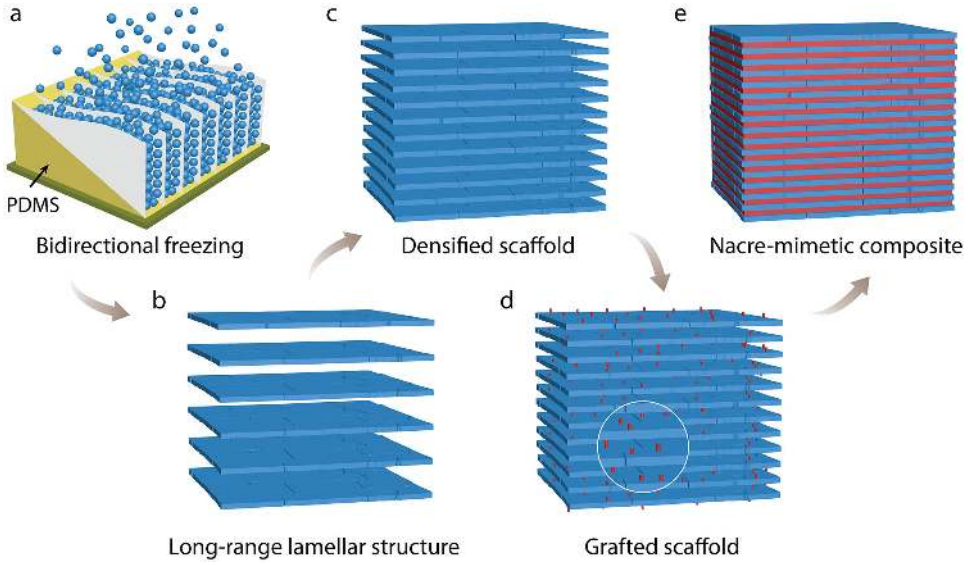

Figure 1. Schematic illustration of fabrication of HA/PMMA composite with nacre-mimetic structure. a) A scaffold was first fabricated by bidirectional freezing of a hydroxyapatite (HA) slurry (20 vol% ceramic loading) on top of a copper cold finger. The presence of the PDMS wedge between the slurry and cold finger causes ice crystals, having nucleated at the base of the wedge, to grow preferentially along the wedge under dual temperature gradients. b) After sublimation and sintering, an HA scaffold with long-range lamellar structure was achieved (porosity is ≈70%). c) The scaffold was further densified by uniaxial pressing to ≈15%–25% porosity. d) Methacrylate groups were grafted onto the HA surface to enhance ceramic–polymer interface. e) A nacre-mimetic composite was finally obtained by in situ polymerization of MMA within the grafted scaffold.

a structural ceramic, but was chosen here due to its well-documented combination with PMMA.[21,22] Having said that, these properties make this composite an outstanding candidate as a bone substitute in orthopedic applications when compared to similar HA-based composites reported in literature, which show at best a maximum HA volume of ≈50%, an elastic modulus of 13 GPa with a bending strength of 92 MPa.[24–34] However, we believe that the design principles and processing strategies utilized here can be transferred to more structural composites, where a higher level of control over structure is required.

The fabrication process used to make our nacre-mimetic HA/PMMA composites is illustrated in **Figure 1**. First, an HA scaffold with long-range aligned lamellar structure was fabricated using a bidirectional freezing method.[22] A 20 vol% HA slurry was placed in a mold on top of a copper cold finger covered by a PDMS wedge (Figure 1a); the wedge generated a horizontal temperature gradient, perpendicular to the vertical gradient from the cold finger. As lamellar ice crystals grew preferentially along the dual temperature gradients, HA particles were expelled from the freezing slurry into the space between the crystals in a similar lamellar pattern. The frozen ice crystals were then sublimated out, leaving behind a porous HA scaffold that was sintered at 1300 °C for 4 h (Figure 1b). As the scaffolds exhibited some 70% porosity, i.e., their ceramic volume fraction was only ≈30% (**Figure 2**a), they were subsequently uniaxially pressed to increase the mineral density (Figure 1c); the resulting densified scaffolds had ≈15%–25% porosity to give a desired ceramic content of ≈75–85 vol%. This process also served to break up the lamellar structure into separate bricks, mimicking nacre's "brick-and-mortar" architecture but without the "mortar" (Figure 2b,c). As it is known that the interface between the ceramic bricks and compliant layer is crucial for the mechanical properties of these composites,[2] the densified scaffold was further grafted with 3-(trimethoxysilyl)propyl methacrylate (γ-MPS) (Figure 1d), to allow the methacrylate groups to further react with monomer during the successive infiltration step and strengthen the interfaces. The final step in creating the nacre-mimetic HA/PMMA composite involved infiltrating the grafted HA scaffold with methyl methacrylate (MMA) which was in situ polymerized into PMMA (Figure 1e).

Figure 2 highlights the strong similarities between the as-prepared HA/PMMA composite and natural nacre. The unpressed HA scaffold contains a long-range aligned lamellar structure (Figure 2a) that resulted from bidirectional freezing; this is very difficult to achieve by conventional freeze casting.[22] After uniaxial pressing, the HA scaffold was largely densified with the lamellar layers broken into separate ceramic "bricks" measuring ≈5–20 μm thick and ≈10–110 μm long (Figure 2b,c). The final HA/PMMA composites, obtained by infiltrating the densified porous scaffolds with PMMA, displayed a hierarchical architecture (with 75–85 vol% ceramic content) over several length-scales in the image of nacre (Figure 2d,e).[4] Specifically, the inorganic bricks can be seen to be parallel, closely packed, and homogeneous throughout the whole sample due to the bidirectional freezing method. The asperities and roughness of the bricks further mimic the inorganic bridges between aragonite platelets found in nacre. Each layer of bricks is separated by polymer layers with thicknesses ranging from submicrometer to several micrometers (Figure 2d). All these structural features are critical for the mechanical performance found in nacre.[6,35]

Three-point bending tests were performed to evaluate the strength, stiffness, and work of fracture of the HA/PMMA composite. The flexural strength increased from 68.6 to 119.7 MPa as the HA content was raised from 72% to 84% (**Figure 3**a). On average for samples with ≈75–85 vol% HA, the ultimate strength was found to be 100.8 ± 8.1 MPa (the maximum

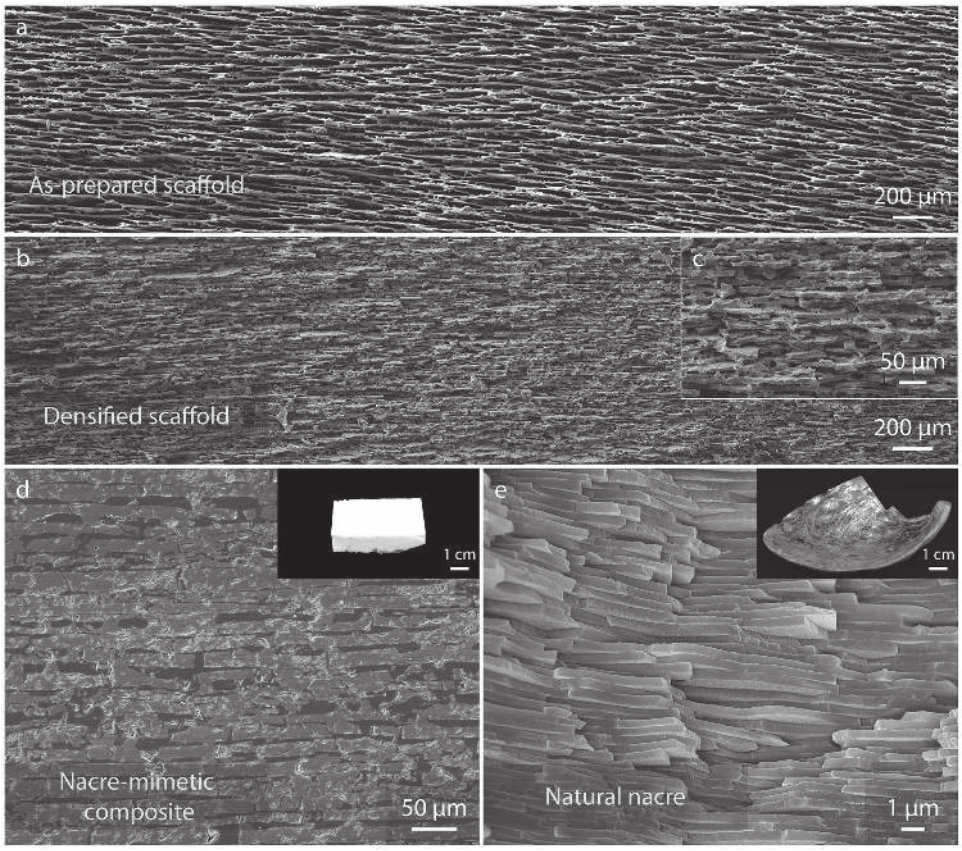

Figure 2. Structure of nacre-mimetic HA/PMMA composite compared to natural nacre. SEM images of a) HA scaffold prepared by bidirectional freezing, and b,c) densified scaffold by uniaxial pressing. d) HA/PMMA composite fabricated by bidirectional freezing and in situ polymerization shows a similar "brick-and-mortar" structure as e) in natural nacre. (Note that the images in (d) and (e) are intended to highlight similarities in structure, but have somewhat different magnifications.)

measured value was 120 MPa), with an elastic modulus of $E = 20.5 \pm 3.9$ GPa (see the Experimental Section below for further details on these measurements). As noted above, such a combination of mechanical properties is superior to other HA-polymer composites reported in the literature,[24–34] with typically 50%–70% higher ceramic content (by volume), ≈10% higher bending strength, and over 50% higher stiffness (in terms of the elastic modulus).

The corresponding work of fracture of the HA/PMMA composite was measured by determining the area under the load–displacement curve and dividing by the area of the fracture surface (Figure 3b). Crack-propagation behavior was also observed in situ inside a scanning electron microscope (SEM); this permitted real time observation of the crack path and its interaction with the microstructure during the measurement of the toughness (Figure 3c–h). Results of samples with 72–84 vol% of HA show that the work of fracture of the composite was nominally inversely related to the ceramic content and ranged from 265 to 2075 J m^{-2} depending on the HA vol%. Even the lowest work of fracture of our composite is still on the order of magnitude larger than the highest of monolithic HA, which is extremely brittle and fails catastrophically at a value of 2.3–20 J m^{-2}.[23] This marked increase in work of fracture in the HA/PMMA material, as compared to monolithic HA, can be ascribed to extensive crack deflection that was observed at the ceramic/polymer interfaces (Figure 3c–e), together with multiple other extrinsic toughening phenomena. These include stretching and tearing in the polymeric "mortar" layers (Figure 3f), where the remaining polymer film can serve as a ligament bridge spanning the crack to carry load that would otherwise be used to propagate the crack, and additional crack bridging and subsequent "pull-out" of the ceramic "bricks" (Figure 3c,d). As in natural nacre,[6,35] in general, the damage was not localized at the crack tip but rather was widely distributed ahead of the growing crack, as indicated by yellow arrows in Figure 3g. Indeed, as the toughness for crack initiation in any ceramic material cannot be readily increased, the prime characteristic of these bioinspired hybrid ceramic materials is that such extrinsic toughening mechanisms provide the means to induce stable (subcritical) crack growth (Figure 3c–e), instead of the unstable (catastrophic) cracking characteristic of most monolithic ceramics such as monolithic HA. The consequent development of extrinsic toughening[36] which permits the occurrence of subcritical cracking growth prior to outright fracture is thus the key feature underlying the potential damage tolerance of these HA/PMMA composite materials.

While the prime rationale for this work was to examine the scientific design principles and processing strategies to develop damage-tolerant lightweight structural materials with higher stiffness, strength, and work of fracture than their

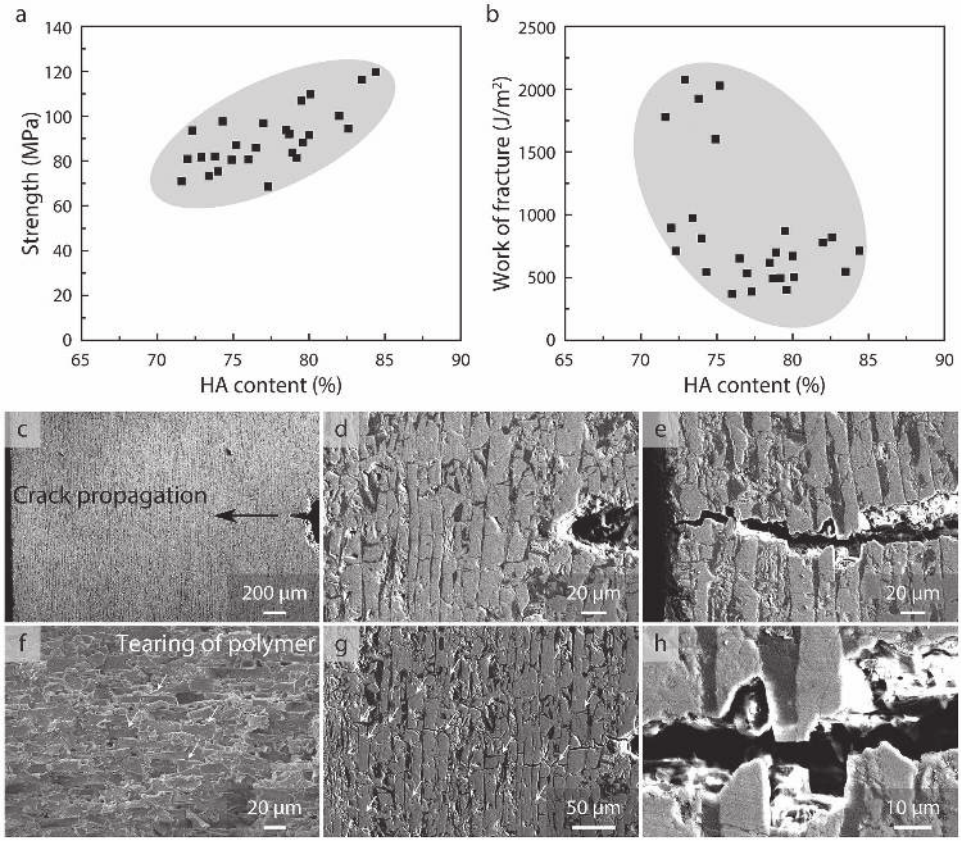

Figure 3. Mechanical properties of HA/PMMA composite with nacre-mimetic structure. a,b) Three-point bending tests were performed to evaluate the strength, stiffness, and work of fracture of the HA/PMMA composite. a) As HA content was raised from 72% to 84%, the flexural strength measured from three-point bending increased from 69 to 120 MPa, while b) the work of fracture decreased from 2075 to 739, with a minimum of 265 J m^{-2}. c–e) Representative SEM images taken during the in situ imaging of the HA/PMMA composite under loading in bending. The "brick-and-mortar" structure, with strong ceramic/polymer interfaces resulting from grafting, promotes various extrinsic toughening mechanisms that stabilize subcritical crack growth instead of the catastrophic fracture that is characteristic of monolithic HA. f) Fracture surface of the HA/PMMA composite with nacre-mimetic structure shows extensive tearing of the PMMA layers (highlighted by white arrows). g) Wide distribution of damage in the form of microcracking within the ceramic layers (highlighted by white arrows). h) "Pull out" between ceramic bricks causes significant tearing of polymer layers.

corresponding (monolithic) ceramic constituents, the current HA/PMMA composites do offer an additional potential as a new bone substitute for orthopedic applications. Bone is the second most transplanted tissue with 2.2 million bone-grafting procedures performed annually worldwide[37,38] As both autografting and allografting[39,40] have significant limitations, such as donor-site morbidity, the possible transmission of diseases, and limited supply, there is high demand for customized bone substitutes to treat bone defects;[37] unfortunately, many currently used ceramic and metallic implant materials have serious shortcomings as they can lack biocompatibility and their physical properties are mismatched to those of bone (**Figure 4**a).[31,37,41,42] In contrast, the current nacre-mimetic HA/PMMA composite displays remarkably similar mechanical properties to natural cortical bone, with a comparable strength of ≈100 MPa and more importantly a stiffness of $E \approx 20$ GPa (Figure 4a), which would act to limit stress shielding of the bone by the implant.

Additionally, slurries containing both HA and PMMA are widely used as bone cement due to their bioactivity and ease of processing.[31] High HA content is required to obtain satisfactory osteoconductivity and mechanical properties in the composite. Moreover, as the polymerization of MMA is an exothermic reaction, lower MMA, i.e., higher HA content, is desired for in vivo polymerization. However, a higher HA content is usually difficult to achieve in such a composite while maintaining its mechanical strength;[41–43] as noted, regular HA-polymer composites described in the literature possess typically only 50 vol% of HA.[3,34,43] In this regard, the present nacre-mimetic HA/PMMA composite appears to be distinctly superior to previous HA/polymer composites that have been developed, in terms of ceramic content and the critical structural properties of stiffness, strength, and work of fracture (Figure 4b,c).[24–34] Akin to nacre, the subtle organization of multiple-scale architectures induces the improved mechanical properties of these composites.

In conclusion, we have fabricated bioinspired hydroxyapatite/PMMA composites with nacre-like "brick-and-mortar" architectures using a bidirectional freeze-casting method, with subsequent surface modification and in situ polymerization. The resulting composites have a relatively high ceramic content (≈75%–85%), strength and elastic stiffness

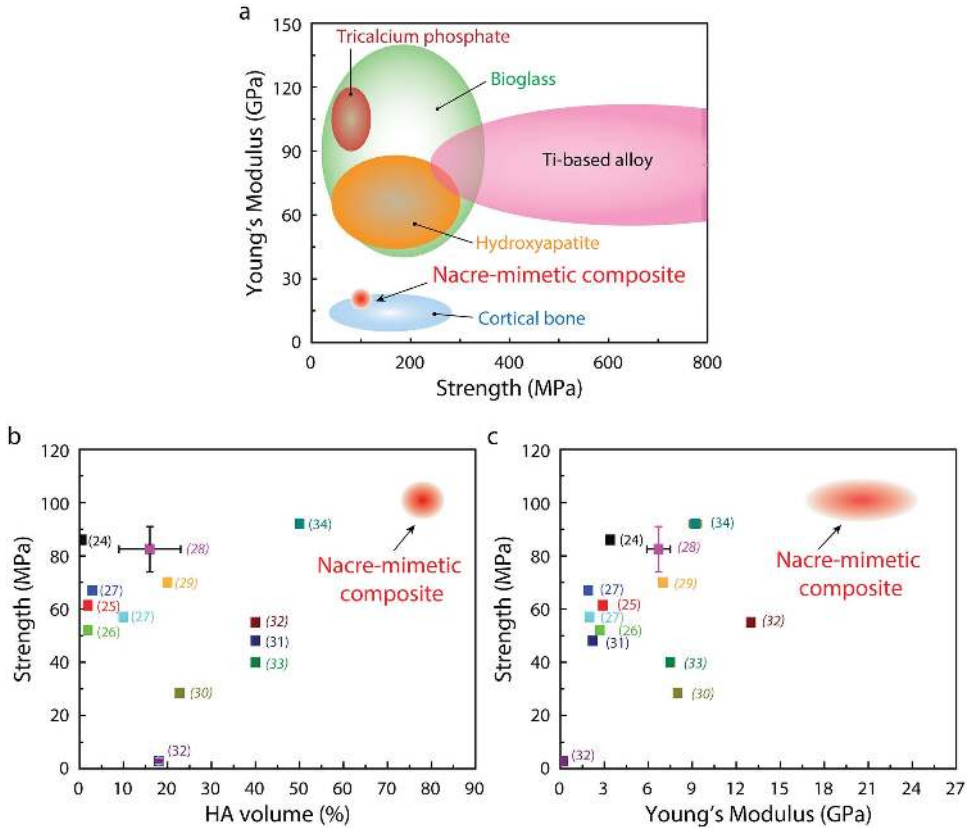

Figure 4. Comparison of nacre-mimetic HA/PMMA composite with other HA-polymer composites and commonly used implant materials.[24–34] a) The mismatch (in Young's modulus and strength) between commonly used implants (bioceramics, bioglass, and titanium-based alloys) and cortical bone. The as-prepared nacre-mimetic HA/PMMA composite has similar modulus and strength with cortical bone, rendering it a good candidate for a bone implant. b,c) In HA-polymer composites, ceramic content and strength are generally inversely correlated. With a "brick-and-mortar" structure, the nacre-mimetic composite can reach as high as ≈85 vol% of ceramic while maintaining exceptional b) strength and c) modulus. An italic reference number indicates that the strength value came from a tensile test; the rest are from flexural tests.

of, respectively, ≈100 MPa and ≈20 GPa, with work of fracture values of 265–2075 J m^{-2}, which are substantially better, by typically one to two orders of magnitude, than monolithic HA (2.3–20 J m^{-2},[23] depending upon the HA vol%. Because of their "brick-and-mortar" architectures, the HA/PMMA composites generate multiple mechanisms of extrinsic toughening that inhibit unstable catastrophic fracture by stabilizing the initial subcritical growth of cracks. While these hybrid microstructures were designed and processed as a model material for strong and lightweight structural ceramics, in their present form the resulting bioinspired HA/PMMA composites do provide a promising new bone substitute material for orthopedic applications. With respect to other ceramic systems, we have successfully fabricated similar scaffolds with mullite and alumina platelet slurries, which demonstrate the potential of this processing technique for other materials.

Experimental Section

Preparation of Scaffold with Long-Range Aligned Lamellar Structure by Bidirectional Freezing of Hydroxyapatite Slurry: Long-range aligned lamellar structures were prepared by bidirectional freezing of a hydroxyapatite slurry (20 vol% ceramic content) above a PDMS wedge on a cooling stage.[22] The slurry was prepared by mixing distilled water with hydroxyapatite powders (density = 3.15 g cm^{-3}, d50 (median particle) size = 2.424 μm, 20 vol%) (Hydroxyapatite #30, Trans-Tech, Adamstown, MD), 1 wt% of Darvan 811 (R. T. Vanderbilt Co., Norwalk, CT), 1 wt% of poly(ethyl glycol) (PEG-300, Sigma-Aldrich), and 2 wt% of an aquazol polymer (ISP) with a molecular weight of 50 000 g mol^{-1}. The slurry was ball-milled for at least 24 h and de-aired in a vacuum desiccator before freezing. The slurry was then poured into a square plastic mold (18 × 18 × 40 mm) with a PDMS wedge at the bottom. This was placed on a copper cold finger connected to a liquid nitrogen reservoir. During the freezing process, lamellar ice crystals grew preferentially under dual temperature gradients, i.e., a vertical gradient away from the cooling stage and a horizontal gradient from the thinner end to the thicker end of the PDMS wedge, generating a long-range aligned lamellar structure. Simultaneously, HA particles were expelled and assembled to replicate the structure of ice crystals. Frozen samples were sublimated (–50 °C, below 0.035 mbar, Freeze Dryer 8, Labconco, Kansas City, MI) for over 48 h and sintered at 1300 °C for 4 h (Air furnace: 1216BL, CM Furnaces Inc., Bloomfield, NJ).

Nacre-Mimetic Composite by Infiltrating HA Scaffold with Poly(methyl methacrylate): The as-prepared scaffold with its long-range aligned lamellar structure was first modified with γ-MPS by immersing the sample into a 1 wt% γ-MPS/ethanol solution for 24 h. Following such a grafting process, the scaffold was dried at 80 °C for 2 h and infiltrated through in situ polymerization of MMA (Sigma-Aldrich) initiated by 0.5 wt% of 2,2-azobisisobutyronitrile (AIBN, Sigma-Aldrich) at 40 °C. After 24 h, the composite was treated at 90 °C for another 2 h to guarantee full polymerization.

Characterization of Nacre-Mimetic Composites: SEM images were obtained using a field-emission scanning electron microscopy (JSM-5700F, JEOL, Japan) at an acceleration voltage of 15 kV in secondary electron mode. Samples were first coated by sputtering with gold at 30 mA for 60 s.

Mechanical Tests on Nacre-Mimetic Composites: Mechanical properties were evaluated by three-point bending on a standard screw-driven mechanical testing machine (Instron 5944 testing system, USA). The strength, elastic modulus,[44,45] and work of fracture properties were measured at a displacement rate of ≈0.015 mm s^{-1} on unnotched, nominally flaw-free (≈2 × 2 × 20 mm) beams that were cut and lightly polished; tests were performed with end-to-end loading spans of 20 mm; sample surfaces were polished to a 1 μm finish using SiC paper. From the resulting load/displacement curves, the strength was measured in terms of the peak load, the stiffness from the slope of the elastic loading line, and the work of fracture from the area under the load/displacement curve normalized by the area of the fracture surface.

To examine the path of the crack until failure, micro-notched bending beams (≈2 × 4.5 × 20 mm) were tested in situ inside a low-pressure Hitachi S-4300SE/N (Hitachi America, Pleasanton, CA, USA) scanning electron microscope using a Gatan MicroTest 2 kN bending stage (Gatan, Abingdon, UK). These samples were first notched using a low-speed saw to a depth of ≈2.25 mm, with the notch root subsequently sharpened (to a root radius of ≈10 μm or less) with a razor blade coated in a 6 μm diamond paste, and then tested in three-point bending with a 16 mm end-to-end loading span at a displacement rate of 0.55 μm s^{-1}.

Acknowledgements

This work was supported by the Mechanical Behavior of Materials Program at the Lawrence Berkeley National Laboratory, funded by the U.S. Department of Energy, Office of Science, Office of Basic Energy Sciences, Materials Sciences and Engineering Division, under Contract No. DE-AC02-05CH11231. The authors would like to thank James Wu, Grace Lau, David Don Lopez, and Dr. Xu Deng for helpful discussions and assistance with the experiments.

Received: September 2, 2015
Revised: September 27, 2015
Published online: November 10, 2015

[1] U. G. Wegst, H. Bai, E. Saiz, A. P. Tomsia, R. O. Ritchie, *Nat. Mater.* **2015**, *14*, 23.
[2] L. J. Bonderer, A. R. Studart, L. J. Gauckler, *Science* **2008**, *319*, 1069.
[3] R. M. Erb, R. Libanori, N. Rothfuchs, A. R. Studart, *Science* **2012**, *335*, 199.
[4] S. Deville, E. Saiz, R. K. Nalla, A. P. Tomsia, *Science* **2006**, *311*, 515.
[5] E. Munch, M. E. Launey, D. H. Alsem, E. Saiz, A. P. Tomsia, R. O. Ritchie, *Science* **2008**, *322*, 1516.
[6] P.-Y. Chen, J. McKittrick, M. A. Meyers, *Prog. Mater. Sci.* **2012**, *57*, 1492.
[7] A. R. Studart, *Adv. Mater.* **2012**, *24*, 5024.
[8] R. O. Ritchie, *Nat. Mater.* **2011**, *10*, 817.
[9] M. A. Meyers, J. McKittrick, P.-Y. Chen, *Science* **2013**, *339*, 773.
[10] Z. Tang, N. A. Kotov, S. Magonov, B. Ozturk, *Nat. Mater.* **2003**, *2*, 413.
[11] P. Podsiadlo, A. K. Kaushik, E. M. Arruda, A. M. Waas, B. S. Shim, J. D. Xu, H. Nandivada, B. G. Pumplin, J. Lahann, A. Ramamoorthy, N. A. Kotov, *Science* **2007**, *318*, 80.
[12] J. Wang, Q. Cheng, Z. Tang, *Chem. Soc. Rev.* **2012**, *41*, 1111.
[13] H.-B. Yao, H.-Y. Fang, X.-H. Wang, S.-H. Yu, *Chem. Soc. Rev.* **2011**, *40*, 3764.
[14] Q. Cheng, L. Jiang, Z. Tang, *Acc. Chem. Res.* **2014**, *47*, 1256.
[15] Q. Cheng, J. Duan, Q. Zhang, L. Jiang, *ACS Nano* **2015**, *9*, 2231.
[16] W. J. Clegg, K. Kendall, N. M. Alford, T. W. Button, J. D. Birchall, *Nature* **1990**, *347*, 455.
[17] G. Dwivedi, K. Flynn, M. Resnick, S. Sampath, A. Gouldstone, *Adv. Mater.* **2015**, *27*, 3073.
[18] F. Bouville, E. Maire, S. Meille, B. Van de Moortele, A. J. Stevenson, S. Deville, *Nat. Mater.* **2014**, *13*, 508.
[19] V. Naglieri, B. Gludovatz, A. P. Tomsia, R. O. Ritchie, *Acta Mater.* **2015**, *98*, 141.
[20] E. Munch, E. Saiz, A. P. Tomsia, S. Deville, *J. Am. Ceram. Soc.* **2009**, *92*, 1534.
[21] F. Bouville, E. Portuguez, Y. Chang, G. L. Messing, A. J. Stevenson, E. Maire, L. Courtois, S. Deville, H. Chan, *J. Am. Ceram. Soc.* **2014**, *97*, 1736.
[22] H. Bai, Y. Chen, B. Delattre, A. P. Tomsia, R. O. Ritchie, *Sci. Adv.* **2015**, *1*, in press.
[23] W. Suchanek, M. Yoshimura, *J. Mater. Res.* **1998**, *13*, 94.
[24] Q. L. Hu, B. Q. Li, M. Wang, J. C. Shen, *Biomaterials* **2004**, *25*, 779.
[25] W. L. Tham, W. S. Chow, Z. A. M. Ishak, *J. Appl. Polym. Sci.* **2010**, *118*, 218.
[26] W. L. Tham, W. S. Chow, Z. A. Mohd Ishak, *J. Reinf. Plast. Compos.* **2010**, *29*, 2065.
[27] S. M. Zebarjad, S. A. Sajjadi, T. E. Sdrabadi, S. A. Sajjadi, A. Yaghmaei, B. Naderi, *Engineering* **2011**, *3*, 795.
[28] R. A. Sousa, R. L. Reis, A. M. Cunha, M. J. Bevis, *Compos. Sci.* **2003**, *63*, 389.
[29] M. S. Abu Bakar, P. Cheang, K. A. Khor, *Compos. Sci.* **2003**, *63*, 421.
[30] L. Fang, Y. Leng, P. Gao, *Biomaterials* **2006**, *27*, 3701.
[31] K. T. Chu, Y. Oshida, E. B. Hancock, M. J. Kowolik, T. Barco, S. L. Zunt, *Biomed. Mater. Eng.* **2004**, *14*, 87.
[32] F. Cruz, *Fabrication of HA/PLLA Composite Scaffolds for Bone Tissue Engineering Using Additive Manufacturing Technologies*, InTech, Rijeka, Croatia **2010**.
[33] M. Younesi, M. E. Bahrololoom, *Mater. Des.* **2009**, *30*, 3482.
[34] N. H. Ladizesky, I. M. Ward, W. Bonfield, *Polym. Adv. Technol.* **1997**, *8*, 496.
[35] A. Y. Lin, M. A. Meyers, *J. Mech. Behav. Biomed. Mater.* **2009**, *2*, 607.
[36] Intrinsic toughening mechanisms operate ahead of the crack tip to generate resistance to microstructural damage. The most prominent mechanism is that of plastic deformation which provides a means of blunting the crack tip through the formation of plastic zones. Extrinsic toughening mechanisms, conversely, operate primarily in the wake of the crack tip to inhibit cracking by "shielding" the crack from the applied driving force. Whereas intrinsic toughening mechanisms are effective in inhibiting both the initiation and growth of cracks, extrinsic mechanisms, e.g., crack bridging and crack deflection, are only effective in providing resistance to crack growth.
[37] P. V. Giannoudis, H. Dinopoulos, E. Tsiridis, *Injury* **2005**, *36*, S20.
[38] A. Van Heest, M. Swiontkowski, *Lancet* **1999**, *353*, S28.
[39] "Autografting" involves transplanting bone from one's own body, whereas "allografting" refers to transplanting bone from another person.
[40] A. P. Jackson, J. F. V. Vincent, R. M. Turner, *Proc. R. Soc. London, Ser. B* **1988**, *234*, 415.
[41] W. Bonfield, *Philos. Trans. R. Soc. A* **2006**, *364*, 227.
[42] S.-H. Kim, B.-K. Lim, F. Sun, K. Koh, S.-C. Ryu, H.-S. Kim, J. Lee, *Polym. Bull.* **2009**, *62*, 111.
[43] J. Zhang, W. Liu, V. Schnitzler, F. Tancret, J. M. Bouler, *Acta Biomater.* **2014**, *10*, 1035.
[44] Measurement of the elastic modulus in bending can be compromised by too small a span-to-depth ratio of the sample, which

has been attributed to an effect of too much shear. To avoid this problem, we have used the maximum loading span possible with the size of samples that were available to us. As a check, law of mixtures' calculations using literature values for the (mechanically measured) modulus of PMMA (≈2–3 GPa) and HA (44–88 GPa) give estimates for the HA/PMMA composite of 20–46 GPa for the range of HA volume fractions studied. We believe, however, that the latter values are likely to be somewhat high as they do not account for the ubiquitous presence of porosity in our materials.

[45] J. A. Johnson, D. W. Jones, *J. Mater. Sci.* **1994**, *29*, 870.